

Classification of Levees using Polarimetric Synthetic Aperture Radar (SAR) Imagery

Lalitha Dabbiru⁽¹⁾, James V. Aanstoos⁽¹⁾, Nicolas H. Younan⁽²⁾

⁽¹⁾ Geosystems Research Institute, Mississippi State University, Box 9627, Mississippi State, MS 39762, USA

⁽²⁾ Department of Electrical and Computer Engineering, Mississippi State University, Mississippi State, MS 39762, USA

Abstract—The recent catastrophe caused by hurricane Katrina emphasizes the importance of examination of levees to improve the condition of those that are prone to failure during floods. On-site inspection of levees is costly and time-consuming, so there is a need to develop efficient techniques based on remote sensing technologies to identify levees that are more vulnerable to failure under flood loading. This research uses NASA JPL’s Uninhabited Aerial Vehicle Synthetic Aperture Radar (UAVSAR) backscatter data for classification and analysis of earthen levees. The overall purpose of this research is to detect the problem areas along the levee such as through-seepage, sand boils and slough slides. This paper focuses on detection of slough slides. Since the UAVSAR is a quad-polarized L-band ($\lambda = 25$ cm) radar, the radar signals penetrate into the soil which aids in detecting soil property variations in the top layer. The research methodology comprises three steps: initially the SAR image is classified into three scattering components using the Freeman-Durden decomposition algorithm; then unsupervised classification is performed based on the polarimetric decomposition parameters: entropy (H) and alpha (α); and finally reclassified using the Wishart classifier. A 3x3 coherency matrix is calculated for each pixel of the radar’s compressed Stokes matrix multi-look backscatter data and is used to retrieve these parameters. Different scattering mechanisms like surface scattering, dihedral scattering and volume scattering are observed to distinguish different targets along the levee. The experimental results show that the Wishart classifier can be used to detect slough slides on levees.

Keywords- backscatter, levee failure, synthetic aperture radar

I. INTRODUCTION

Monitoring the physical condition of levees is vital in order to protect them from flooding. The dynamics of subsurface water events can cause damage on levee structures which could lead to slough slides, sand boils or through seepage. Physical inspection of levees to detect the problem areas is time consuming and expensive. Synthetic Aperture Radar (SAR) technology, due to its high spatial resolution and soil penetration capability, is a good choice to identify such problem areas so that they can be treated to avoid possible catastrophic failure.

The radar backscatter data is capable of identifying variations in soil properties of the areas which might cause levee failure. In this research we analyzed Uninhabited Aerial Vehicle Synthetic Aperture Radar (UAVSAR) backscatter data to observe levees along the lower Mississippi river. Each

pixel in the radar image represents the radar backscatter for that area on the ground; bright features mean that a large fraction of energy was reflected back to the radar, while dark features imply that very little energy was reflected. Backscatter will also differ depending on the use of different polarizations. UAVSAR transmits pulses in horizontal (H) and vertical (V) polarization and receives in both H and V, with the resultant combinations of HH (Horizontal transmit, Horizontal receive), VV (Vertical transmit, Vertical receive), HV (Horizontal transmit, Vertical receive) or VH (Vertical transmit, Horizontal receive). Such polarimetric SAR (PolSAR) data has been used to retrieve a variety of useful information such as land cover, land use and soil moisture.

UAVSAR was developed by NASA’s Jet Propulsion Laboratory (JPL) for acquiring repeat track SAR data. It provides differential interferometric measurements to estimate surface deformation. The key parameters of the UAVSAR instrument are given in Table 1 [1].

TABLE I
UAVSAR INSTRUMENT KEY PARAMATERS

Parameter	Value
Frequency	L- Band (1.26 GHz)
Bandwidth	80 MHz
Range Resolution	1.8 m
Polarization	Quad Polarization
Raw ADC Bits	12 baseline
Range Swath	16 km
Look Angle Range	25° - 60°
Transmit Power	> 2.0 KW
Altitude Range	2000 – 18000 m

Interferometric Synthetic Aperture Radar (INSAR) technology has been in use to characterize land subsidence

problems in the regions of Coachella Valley, California to measure land surface changes by using interferograms [2]. Cloude and Pottier [3] [6] developed a polarimetric decomposition theorem based on the eigenvector analysis of the coherency matrix calculated for each pixel and it is used to retrieve three important parameters: entropy (H), scattering angle (α) and anisotropy (A). By interpreting the analysis as a measure of entropy and scattering angle, the classification of the scene can be made into nine scattering zones. Lee et al. [4] derived a distance measure based on complex Wishart distribution between a coherency matrix and a cluster mean of each class for multi-look polarimetric SAR data. The unsupervised Wishart classification proposed by them is based on the Cloude-Pottier H/alpha classification. Later, the fuzzy c-means algorithm was applied to address inherent vagueness of the class boundaries [5]. Freeman and Durden [7] developed unsupervised classification algorithms which provide information on the terrain scatter type. The algorithm separates the image into three classes: surface, double-bounce and volume scattering classes. These backscattering properties of the target are described by a scattering matrix S [8] which represents the reflectivity of the area being observed at a given radar wavelength.

$$\text{Scattering Matrix } S = \begin{bmatrix} S_{hh} & S_{hv} \\ S_{vh} & S_{vv} \end{bmatrix} \quad (1)$$

where h indicates horizontal polarization and v indicates vertical polarization.

The scattering matrix is vectorized using Pauli spin elements to obtain the coherency matrix which is shown below [3].

$$\text{Scattering Matrix } \vec{K}_p = \frac{1}{\sqrt{2}} \begin{bmatrix} S_{hh} + S_{vv} \\ S_{hh} - S_{vv} \\ 2S_{hv} \end{bmatrix} \quad (2)$$

$$(S_{hv} = S_{vh} \text{ due to symmetry})$$

The coherency matrix is a 3 x 3 hermitian matrix generated by the outer product of \vec{K}_p vector with its conjugate transpose and is given by:

$$\text{Coherency Matrix } [T] = \vec{K}_p \cdot \vec{K}_p^{*T} \quad (3)$$

where * and T represent complex conjugate and transpose respectively. The three diagonal elements of the coherency matrix correspond to surface, double bounce and volume scattering components of the data. The decomposition parameters entropy (H), alpha (α) and anisotropy (A) are extracted from the coherency matrix [3] [6]. The parameter entropy (H) indicates the degree of randomness of the scattering medium, the anisotropy parameter is to discriminate scattering mechanisms with different eigenvalue distributions and the parameter α is an indicator of dominant scattering mechanism [9]. These parameters are defined as:

$$\text{Entropy } H = -\sum_{i=1}^3 p_i \log_3(p_i) \quad (4)$$

$$\text{where } p_i = \frac{\lambda_i}{\sum_{k=1}^3 \lambda_k}$$

where p_i corresponds to the pseudo-probabilities obtained from the eigenvalues λ_i .

The anisotropy parameter measures the importance of the second and third eigenvalues of the eigen decomposition and is given by:

$$\text{Anisotropy } A = \frac{\lambda_2 - \lambda_3}{\lambda_2 + \lambda_3} \quad (5)$$

The parameter α is an indicator of scattering mechanism, which ranges from 0 to 90°.

$$\alpha = \sum_{i=1}^3 (p_i \alpha_i) \quad (6)$$

II. STUDY AREA AND DATA USED

The area of concentration is along the levees of the lower Mississippi river which passes through the states of Mississippi, Louisiana and Arkansas as outlined in Fig. 1.

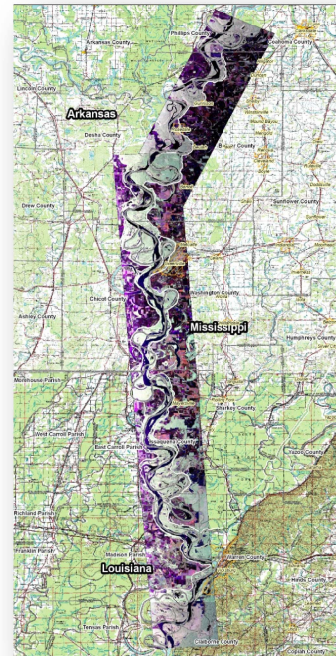


Fig. 1. Location of the study area

NASA JPL's UAVSAR flew twice over the study area to acquire imagery and the total study area was covered by two flight lines; one being the 178 km flight line and the other being a 64 km flight line. The quad-polarized L-band data

from the instrument was pre-processed at JPL. From the raw data of each flight line, three Single-Look Complex (SLC) slant range imagery, six Multi-Look Cross-Product (MLC) slant range imagery, six ground range projected (GRD) files and one data (DAT) file were generated for the radar image processing. The SLC imagery has the highest spatial resolution but also has a lot of speckle noise. So the MLC files were derived from the average of the product of each SLC pixel, 3 pixels in the range and 12 pixels in the azimuth direction. The data file is a compressed Stokes matrix of multi-looked data containing 10 bytes of information per pixel, with two bytes used to store the total power.

III. EXPERIMENTAL RESULTS

NASA JPL's L-Band UAVSAR data acquired in June 2009 was used to develop the classification scheme. Fig. 2(a) shows the optical image of the study area subset where multiple number of slough slides occurred in the recent past and this area has been chosen for analysis. Based on the *in situ* data, the slides are marked by dots shown in Fig 2(a). A 3x3 coherency matrix is calculated for each pixel of the radar's compressed Stokes matrix multi-look backscatter data. Initially, the Freeman-Durden decomposition algorithm was applied to the study area subset, separating the image into three classes: surface, double-bounce and volume scattering. Fig. 2(b) shows the RGB composite, where the surface scattering is represented in blue, double-bounce scattering is set to red and volume scattering is set to green. According to the three coefficients the dominant scattering can be determined and it is observed that the pixels on the levee within slides have high surface scattering values as shown in Fig 2(c).

Next, the unsupervised H/alpha classification is performed based on the polarimetric target decomposition parameters entropy (H) and scattering angle (α) which are derived from the eigenvalue decomposition of the coherency matrix. The alpha angle corresponds to the variation in scattering mechanism, with $\alpha = 0^\circ$ corresponding to surface scattering, $\alpha = 45^\circ$ dipole scattering, and $\alpha = 90^\circ$ double bounce scattering. For smooth surfaces surface scattering dominates and the entropy is close to 0. The randomness of scattering characteristics in forest areas causes high entropy, whereas the Mississippi river causes low entropy due to its surface (isotropic) scattering. All the pixels in the image were classified into nine zones on the H/alpha plane, characterizing different scattering mechanisms.

Fig. 3 is the result of Wishart unsupervised classification performed on the study area subset. The Wishart classification performs a maximum likelihood segmentation of polarimetric data sets based on the multivariate complex Wishart probability density function [4]. The eight classes which resulted from the H/alpha classification are used to initialize the unsupervised Wishart classification and iteratively refine the clusters. The iteration termination criterion depends on logical combination of two conditions; 1) the number of pixels switching class and, 2) when it reaches the specified number of iterations. In our application the algorithm terminated after

10 iterations with 10 pixels switching class. In this classification result it can be observed that water and bare soil are dominated by surface scattering (Blue color). For surface scattering, S_{HV} is small, S_{HH} and S_{VV} are correlated, and their phase is close to 0 degrees. Since UAVSAR's L-Band instrument has a relatively long wavelength, it penetrates through short vegetation and the backscatter is mostly from the underlying ground. Forest areas produce volume scattering (Green Color), with a small amount of double bounce scattering (Red Color). For volume scattering S_{HV} is large, S_{HH} and S_{VV} are weakly correlated. Double bounce scattering dominates in case of young trees where there is strong backscatter from the leaves and trunks. As seen in Fig. 3 the pixels in the vicinity of slides fall into a different cluster (Orange Color) than the normal levee pixels (Blue Color). Based on the Freeman-Durden decomposition (Fig. 2(c)) we can see that this is due to the higher surface scattering component in the vicinity of slides, probably due to the greater roughness of soil in the slide.

It can be seen that some portions of the levee that are not located near the known slides fall into the same (Orange Color) cluster. While these might simply be "false positives", it may be that the soil at these sites has similar characteristics to that in the slide areas. As such this feature may indicate potential future slides.

IV. CONCLUSIONS AND FUTURE WORK

The eigenvector based H/alpha classification leads to an improved understanding of the scattering mechanisms of the target area. The Wishart classification technique has good potential for detecting slough slides on levees. It may also detect areas of potential future slides, but this hypothesis needs further investigation. For this, we are collecting detailed *in situ* soil measurements of the study area and will compare these with our classification.

Soil moisture variations may indicate differences in soil texture properties that could lead to future levee problems. Therefore we are also investigating the application of radar-based soil moisture estimation algorithms to this work.

We recently acquired high quality X – band radar imagery of our study area from the TerraSAR-X satellite and will determine if it can be successfully used in this application.

ACKNOWLEDGMENT

The authors would like to thank the US Army Corps of Engineers, Engineer Research and Development Center and Vicksburg Levee District for providing ground truth data and expertise.

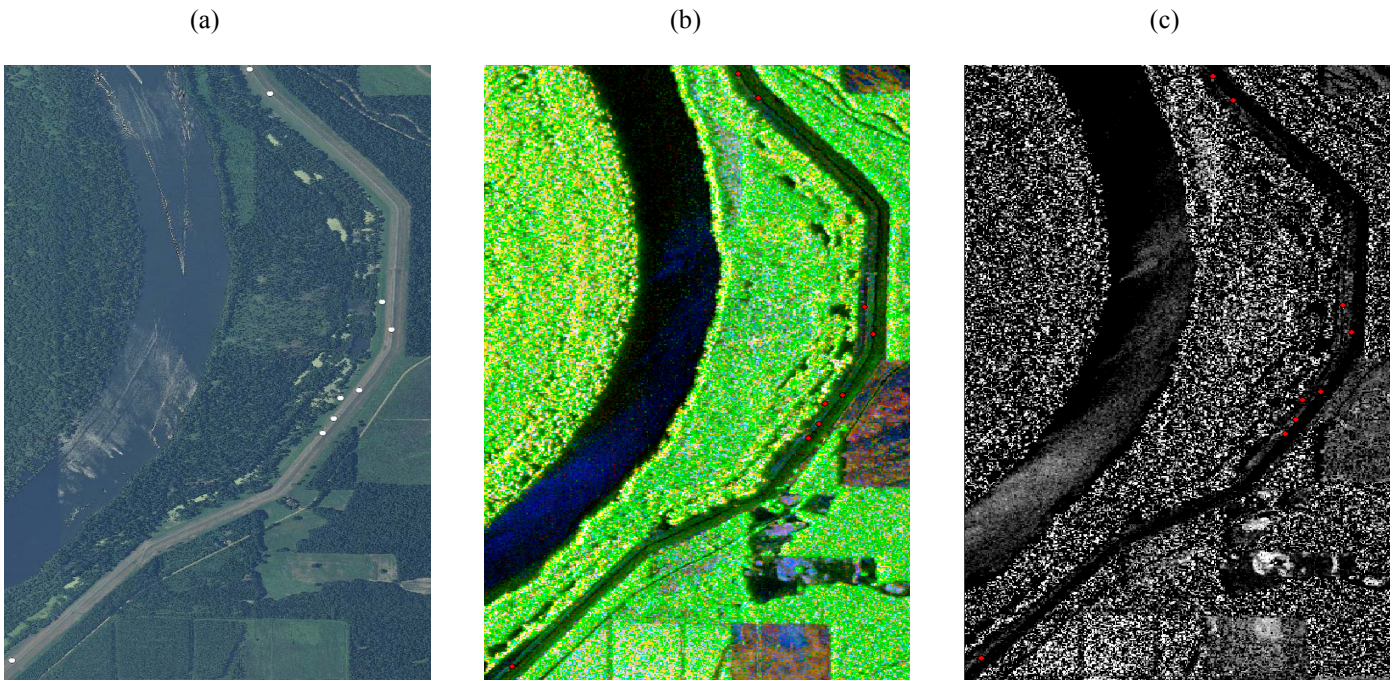


Fig. 2. Application of the Freeman-Durden decomposition algorithm to the L-band UAVSAR data. (a) Optical image of the study area subset, with nine landslides locations marked by dots; (b) RGB composite of the Freeman-Durden decomposition; (c) Surface scattering component.

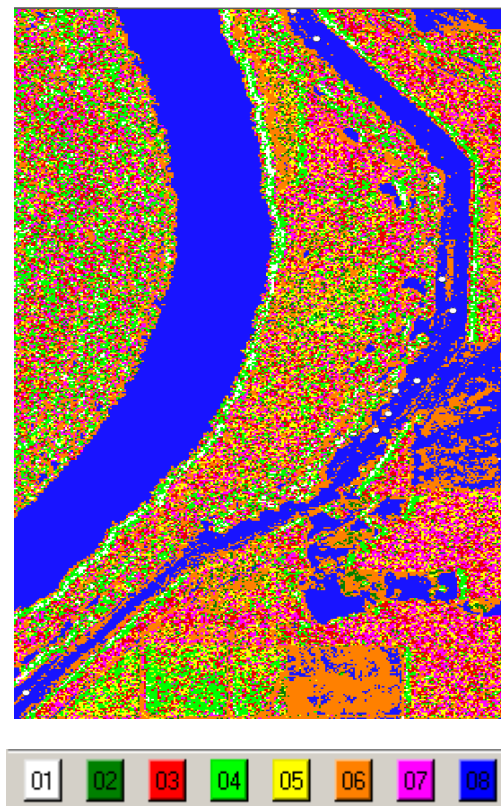


Fig. 3. H/alpha Wishart classification result

REFERENCES

- [1] Paul A. Rosen, Scott Hensley, Kevin Wheeler, Greg Sadowy, Tim Miller, Scott Shaffer, Ron Muellerschoen, Cathleen Jones, Howard Zebker and Soren Madsen, "UAVSAR: A New NASA Airborne SAR System for Science and Technology Research", *IEEE Conference on Radar*, 2006.
- [2] Michelle Sneed, and Justin T. Brandt, "Detection and Measurement of Land Subsidence Using Global Positioning System Surveying and Interferometric Synthetic Aperture Radar, Coachella Valley, California, 1996–2005", *U.S. Geological Survey, Scientific Investigations Report*, 2007–5251.
- [3] Shane Robert Cloude and Eric Pottier, "An entropy based classification scheme for land applications of polarimetric SAR", *IEEE Transactions on Geoscience and Remote Sensing*, vol. 35, No. 1, 1997.
- [4] J.S. Lee, M.R. Grunes, T.L. Ainsworth, L. Du, D.L. Schuler, and S.R. Cloude, "Unsupervised classification using polarimetric decomposition and complex Wishart classifier", *IEEE*, 1998.
- [5] M.Hellmann, G. Jager and E. Pottier, "Fuzzy clustering and interpretation of fully polarimetric SAR data", *IEEE*, 0-7803-7031-1/01, 1996.
- [6] Shane Robert Cloude and Eric Pottier, "A review of target decomposition theorems in radar polarimetry", *IEEE Transactions on Geoscience and Remote Sensing*, vol. 34, No. 2, 1996.
- [7] Anthony Freeman and Stephen L. Durden, "A three-component scattering model for polarimetric SAR data", *IEEE Transactions on Geoscience and Remote Sensing*, vol. 36, No. 3, May 1998.
- [8] J. J. Van Zyl, Howard A. Zebker, and Charles Elachi, "Imaging radar polarization signatures: Theory and observation", *Radio Science*, vol. 22, no. 4, pp. 529-543, 1987.
- [9] Jong-Sen Lee and Eric Pottier, "Polarimetric radar imaging from basics to applications", *CRC Press*, 2009, pp 238.